# Redox Chemistry of $[Co_4(CO)_3(\mu_3\text{-}CO)_3(\mu_3\text{-}C_7H_7)(\eta^5\text{-}C_7H_9)]$ – Reversible Carbon–Carbon Coupling versus Metal Cluster Degradation

**Hubert Wadepohl,*[a] Stefan Gebert,[a] Hans Pritzkow,[a] Domenico Osella,*[b] Carlo Nervi,[c] and Jan Fiedler[d]**

*Dedicated to Professor Heinrich Vahrenkamp on the occasion of his 60th birthday*

**Keywords:** Carbocycles / Clusters / Cobalt / Electrochemistry / Facial ligands

Chemical reduction of the tetracobalt cluster complex $[Co_4(CO)_3(\mu_3\text{-}CO)_3(\mu_3\text{-}C_7H_7)(\eta^5\text{-}C_7H_9)]$ **(3)**, followed by addition of $[PPh_4]Br$, gives the complex $[\{Co_4(CO)_3(\mu_3\text{-}CO)_3(\mu_3\text{-}C_7H_7)\}_2\{\mu\text{-}\eta^4\text{:}\eta^4\text{-}(C_7H_9)_2\}]^{2-}$ as a mixture of two diastereomers $[\mathbf{4A}]^{2-}$ and $[\mathbf{4B}]^{2-}$ in high yield. The crystal structure of $[\mathbf{4A}]^{2-}[PPh_4]_2\cdot 1.5C_7H_8$ has been determined and confirms the reductive coupling of two $Co_4$ cluster coordinated apical cycloheptadienyl rings to form a bridging bicycloheptyl-3,5,3′,5′-tetraene ligand. Reduction of **3** with $Li[HBEt_3]$ and subsequent treatment with aqueous $[NnBu_4]Cl$ results in the formation of $[Co_4(CO)_3(\mu_3\text{-}CO)_3(\mu_3\text{-}C_7H_7)(C_7H_{10})]^-$ $[\mathbf{5}]^-$. Addition of $[(\eta\text{-}C_6H_6)Ru(NCMe)_3][BF_4]_2$ after the borohydride reduction gives $[Ru(\eta\text{-}C_6H_6)Co_3(CO)_3(\mu_3\text{-}CO)_3(\mu_3\text{-}C_7H_7)]$ **(6)**, a product derived from reductive $Co_4$ cluster degradation. A detailed electrochemical and spectro-electrochemical study of the redox behaviour of **3** and $[\mathbf{4}]^{2-}$ has been carried out. The complex potential current response of **3** is rationalized in terms of the formation of the radical anion $[\mathbf{3}]^-$ as the primary intermediate, which may be reversibly reduced further to give the much more stable $[\mathbf{3}]^{2-}$ and then $[\mathbf{3}]^{3-}$. Dimerization of $[\mathbf{3}]^-$ to give $[\mathbf{4}]^{2-}$ occurs by formation of a new carbon–carbon bond between the apical $C_7H_9$ ligands. The two redox-active moieties in $[\mathbf{4}]^{2-}$ behave as independent, non-interacting redox centres. The oxidized form **4** is unstable and dissociates back to **3** almost quantitatively, thus completing a redox cycle characteristic of a "molecular battery". The homogeneous rate constant for dimerization has been evaluated as $k_{DIM}$ ($2\ [\mathbf{3}]^- \rightarrow [\mathbf{4}]^{2-}$) = $0.30 \pm 0.05$ $mM^{-1}\ s^{-1}$.

## Introduction

Two contrasting statements are frequently made concerning the consequences of an electron transfer to or from a molecular metal cluster complex:[1] (i) behaviour of the cluster as an "electron sponge", i.e. the ability to add or lose electrons without any great effect on the framework, and (ii) a rearrangement of the metal core, upon reduction typically involving cleavage of metal–metal bonds. This is usually attributed to the frontier orbitals of the cluster being generally nonbonding or antibonding with respect to the metal–metal interactions. However, as shown, for example, by the frequently observed labilization of ligands[2] at the periphery of the cluster, metal–ligand bonding may also be affected by the electron–transfer process.[3]

Recently, we have reported on the redox behaviour of a series of tetracobalt cluster complexes with a cyclooctatetraene ligand in the unusual facial ($\mu_3$) coordination mode.[4] On chemical reduction, cluster complexes of the

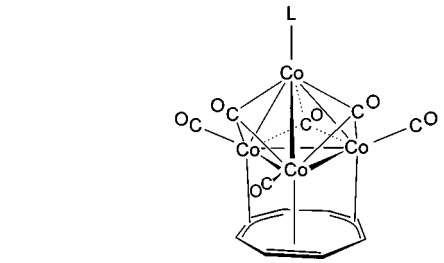


**1**

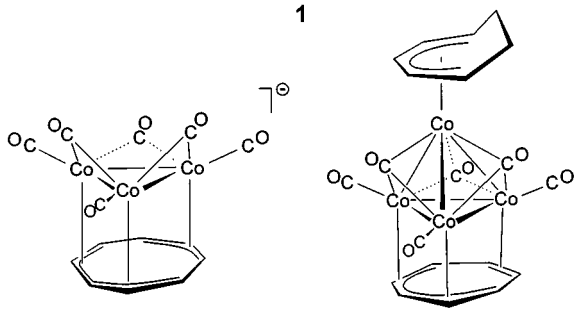

**2** **3**

[a] Anorganisch-chemisches Institut der Ruprecht-Karls-Universität,
Im Neuenheimer Feld 270, D-69120 Heidelberg, Germany
E-mail: bu9@ix.urz.uni-heidelberg.de
[b] Dipartimento di Scienze e Tecnologie Avanzate, Università del Piemonte Orientale "A. Avogadro",
Corso T. Borsalino 54, I-15100 Alessandria, Italy
E-mail: osella@ch.unito.it
[c] Dipartimento di Chimica IFM, Università di Torino,
Via P. Giuria 7, I-10125 Torino, Italy
[d] The J. Heyrovský Institute of Physical Chemistry, Academy of Sciences of the Czech Republic,
Dolejskova 3, 18223 Prague 8, Czech Republic

  1434–1948/00/0808–1833 $ 17.50+.50/0 

type $[Co_4(CO)_3(\mu_3\text{-}CO)_3(\mu_3\text{-}C_8H_8)(L)]$ [**1a**, L = $\eta^4$-$C_8H_8$; **1b**, L = $\eta^4$-$C_6H_8$; **1c**, L = $\eta^4$-diphenylfulvene; **1d**, L = $(CO)_2$][5] are degraded to give the trinuclear cluster anion $[Co_3(CO)_3(\mu_2\text{-}CO)_3(\mu_3\text{-}C_8H_8)]^-$ $[\mathbf{2}]^-$ in high yield. This behaviour follows the general pattern outlined above, but is nevertheless in marked contrast to that of the parent binary carbonyl cluster, $[Co_4(CO)_{12}]$. Here, reduction usually leads to a complete breakdown of the cluster.[6] The trinuclear anion $[Co_3(CO)_{10}]^-$, a close analogue of $[\mathbf{2}]^-$, is quite unstable and can only be obtained from $[Co_4(CO)_{12}]$ under very special conditions.[7]

We report herein on the reduction of $[Co_4(CO)_3(\mu_3\text{-}CO)_3(\mu_3\text{-}C_7H_7)(\eta^5\text{-}C_7H_9)]$ **(3)**,[5] a cluster complex with a facial cycloheptatrienyl ligand. It is shown that the reduction chemistry of this complex is fundamentally different from that of **1**, despite the fact that these systems are isoelectronic and structurally similar.

## Results

### Preparative and Spectroscopic Investigations

Treatment of $[Co_4(CO)_3(\mu_3\text{-}CO)_3(\mu_3\text{-}C_7H_7)(\eta^5\text{-}C_7H_9)]$ **(3)** with either $Li[HBEt_3]$, LiPh, $Na_2[Fe(CO)_4]$, or cobaltocene, followed by addition of $[PPh_4]Br$ and precipitation with methanol gave a >80% yield of the complex $[\{Co_4(CO)_3(\mu_3\text{-}CO)_3(\mu_3\text{-}C_7H_7)\}_2\{\mu\text{-}(C_7H_9)_2\}][PPh_4]_2$ as a mixture of two diastereomers, $[\mathbf{4A}]^{2-}[PPh_4]_2$ and $[\mathbf{4B}]^{2-}[PPh_4]_2$. Complete separation of the two isomers proved to be impossible on a preparative scale. Repeated crystallization from methanol/THF or nitromethane led to an enrichment in one diastereomer in the solid (up to an 86:14 ratio). This complex, $[\mathbf{4A}]^{2-}[PPh_4]_2$, was finally obtained in pure form as a small batch of single crystals by layering a $CH_2Cl_2$ solution of the 86:14 isomeric mixture with toluene. Isomer $[\mathbf{4B}]^{2-}[PPh_4]_2$ was only obtained about 80% pure (containing 20% $[\mathbf{4A}]^{2-}[PPh_4]_2$) from the pooled mother liquors.

Column chromatography of the supernatant solution that was left after the first precipitation with methanol gave a second anion, $[Co_4(CO)_3(\mu_3\text{-}CO)_3(\mu_3\text{-}C_7H_7)(C_7H_{10})]^-$ $[\mathbf{5}]^-$, which was obtained as the $[PPh_4]^+$ salt in very low yield (about 1%). In another experiment, where the reaction product of **3** and $Li[HBEt_3]$ was treated with aqueous $[NnBu_4]Cl$, $[\mathbf{5}]^-$ was isolated after recrystallization from ethanol as the $[NnBu_4]^+$ salt in 26% yield.

The course of the reaction of **3** with $Li[HBEt_3]$ was found to be unaffected by changing the stoichiometric ratio (1−4 equivalents of the reducing agent were used). NMR analysis of the initial reduction product (in $[D_8]$THF) showed only minor resonances in the region $-2 \leq \delta \leq 10$.

In order to trap any more highly reduced species, a THF solution of complex **3** was first treated with $Li[HBEt_3]$. The resulting material was then reacted with $[(\eta\text{-}C_6H_6)Ru(NCMe)_3][BF_4]_2$ in $CH_2Cl_2$. From this reaction, the dark-brown cluster complex $[Ru(\eta\text{-}C_6H_6)Co_3(CO)_3(\mu_3\text{-}CO)_3(\mu_3\text{-}C_7H_7)]$ **(6)** was isolated in 18% yield after column chromatography. On monitoring the reaction by IR spectroscopy, a rapid decrease in the $\nu_{CO}$ bands attributable to the starting material **3** was observed following the addition of the $Li[HBEt_3]$ solution, which was accompanied by a concomitant increase of new broad features at 1950 (sh), 1926 (vs), 1700 (sh), and 1675 (s) $cm^{-1}$. The formation of **6** was seen to be complete within a few minutes after the addition of one equivalent of the ruthenium reagent.

The cluster anions $[\mathbf{4A}]^{2-}$, $[\mathbf{4B}]^{2-}$, and $[\mathbf{5}]^-$, as well as the neutral complex **6**, were characterized by spectroscopic

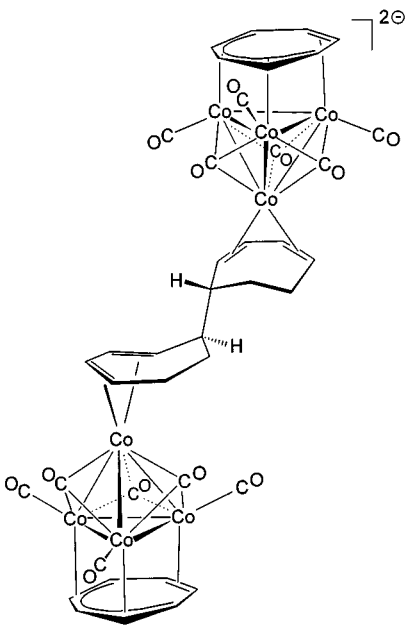


$[\mathbf{4A}]^{2-}$

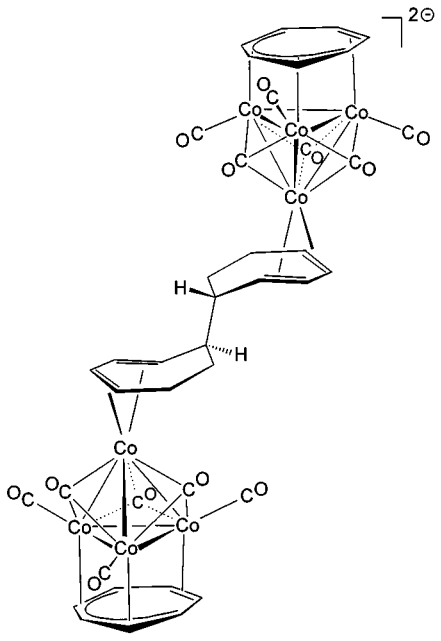


$[\mathbf{4B}]^{2-}$

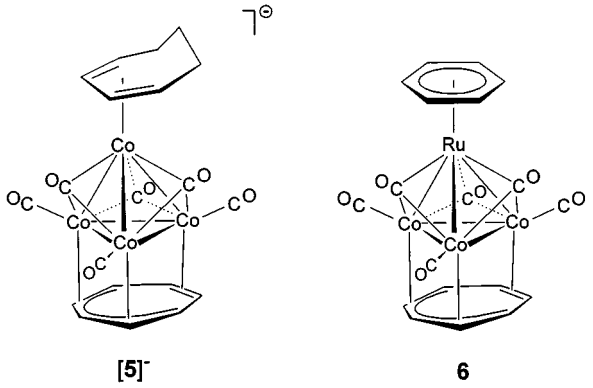


**[5]⁻** **6**

methods, and by a crystal structure analysis of $[\mathbf{4A}]^{2-}[PPh_4]_2$. The infrared ($\nu_{CO}$) spectra of all the anions are quite similar; they consist of two broad features in the characteristic regions for terminal (around 1930 $cm^{-1}$) and triply-bridging carbonyls (around 1680 $cm^{-1}$). Compared to the neutral starting material, the CO stretches are shifted by about 50−60 $cm^{-1}$ to lower frequencies. Due to the broad absorptions, a distinction between the individual species cannot be made. The IR bands of the $Co_3Ru$ complex **6** also appear at slightly lower wavenumbers (about 10−20 $cm^{-1}$) than those of the $Co_4$ cluster **3**. $^1H$ and $^{13}C$ NMR spectroscopic data for $[\mathbf{4A}]^{2-}$ and $[\mathbf{4B}]^{2-}$ are collected in Table 1 and Table 2, along with the corresponding data for $[\mathbf{5}]^-$.

The spectra of **6** are very simple, with just two singlets appearing in both the $^1H$ ($\delta$ = 3.20, 5.35) and $^{13}C$ NMR spectra ($\delta$ = 59.8, 95.6). Due to the low solubility and the long relaxation times of the carbonyls, no $^{13}C$ resonances were detected for these ligands in **6**.

### Molecular Structure of $[\mathbf{4A}]^{2-}$

An X-ray crystal structure determination was carried out on a single crystal of $[\mathbf{4}]^{2-}[PPh_4]_2 \cdot 1.5C_7H_8$, containing the diastereomer $[\mathbf{4A}]^{2-}$. Details of the structure determination are given in the Experimental Section. The crystal structure arises from a packing of octanuclear cluster dianions $[\{Co_4(CO)_3(\mu_3\text{-}CO)_3(\mu_3\text{-}C_7H_7)\}_2\{\mu\text{-}\eta^4\text{:}\eta^4\text{-}(C_7H_9)_2\}]^{2-}$ and tetraphenylphosphonium cations, which are interspersed by a total of three molecules of toluene per unit cell as a solvent of crystallization. Due to the rather poor quality of the single crystals, coupled with inherent disorder in some parts of the structure, the accuracy of the structure determination is limited.

A view of the $[\mathbf{4A}]^{2-}$ molecule is presented in Figure 1. Salient bond lengths are given in Table 3. The complex di-

Table 1. $^1H$ NMR spectroscopic data ($\delta$, in $CD_2Cl_2$) for $[\{Co_4(CO)_3(\mu_3\text{-}CO)_3(\mu_3\text{-}C_7H_7)\}_2\{\mu\text{-}(C_7H_9)_2\}]^{2-}$ $[\mathbf{4}]^{2-}$ and $[Co_4(CO)_3(\mu_3\text{-}CO)_3(\mu_3\text{-}C_7H_7)(C_7H_{10})]^-$ $[\mathbf{5}]^-$

| Complex | $\mu_3$-$C_7H_7$ | $\eta^4$:$\eta^4$-$C_{14}H_{18}$ | |
|---|---|---|---|
| $[PPh_4]_2[\mathbf{4A}]^{2-}$ | 3.48 (s, 14 H) | $CH_2$: | 1.1 (m, 4 H), 1.9 (m, 4 H) |
| | | (CH)bridgehead: | 1.4 (m, 2 H) |
| | | (CH)diene (H-1, H-4): | 3.28 (m, 2 H), 3.4 (m, 2 H)[a] |
| | | (CH)diene (H-2, H-3): | 5.3 (m, 2 H),[a] 5.48 (m, 2 H) |
| $[PPh_4]_2[\mathbf{4B}]^{2-}$ | 3.44 (s, 14 H) | CH2: | 1.1 (m, 4 H), 1.9 (m, 4 H) |
| | | (CH)bridgehead: | 1.4 (m, 2 H) |
| | | (CH)diene (H-1, H-4): | 3.3−3.4 (m, 4 H)[a] |
| | | (CH)diene (H-2, H-3): | 5.3 (m, 2 H),[a] 5.54 (m, 2 H) |
| $[PPh_4][\mathbf{5}]^-$ | 3.50 (s, 7 H) | CH2: | 1.41 (m, 4 H), 1.95 (m, 2 H) |
| | | (CH)diene (H-1, H-4): | 3.4 (m, 2 H)[a] |
| | | (CH)diene (H-2, H-3): | 5.49 (m, 2 H) |

[a] Resonances partially obscured by solvent or $C_7H_7$ resonance.

Table 2. $^{13}C\{^1H\}$ NMR spectroscopic data ($\delta$, in $CD_2Cl_2$) for $[\{Co_4(CO)_3(\mu_3\text{-}CO)_3(\mu_3\text{-}C_7H_7)\}_2\{\mu\text{-}(C_7H_9)_2\}]^{2-}$ $[\mathbf{4}]^{2-}$ and $[Co_4(CO)_3(\mu_3\text{-}CO)_3(\mu_3\text{-}C_7H_7)(C_7H_{10})]^-$ $[\mathbf{5}]^-$; signal multiplicities (due to coupling to $^1H$) were determined by DEPT (135°) spectra and are given as even (e) or odd (o)

| Complex | $\mu_3$-$C_7H_7$ | $\eta^4$:$\eta^4$-C14H18 | | CO |
|---|---|---|---|---|
| $[PPh_4]_2[\mathbf{4A}]^{2-}$ | 56.0 (e) | $CH_2$: | 28.2 (o), 28.5 (o) | 202.5, 280.8 |
| | | (CH)bridgehead: | 45.5 (e) | |
| | | (CH)diene (C-1, C-4): | 70.2 (e), 72.5 (e) | |
| | | (CH)diene (C-2, C-3): | 100.4 (e), 100.5 (e) | |
| $[PPh_4]_2[\mathbf{4B}]^{2-}$ | 56.0 (e) | $CH_2$: | 26.9 (o), 28.5 (o) | 205.5, 280.3 |
| | | (CH)bridgehead: | 45.9 (e) | |
| | | (CH)diene (C-1, C-4): | 70.3 (e), 73.6 (e) | |
| | | (CH)diene (C-2, C-3): | 99.7 (e), 100.9 (e) | |
| $[PPh_4][\mathbf{5}]^-$ | 56.3(e) | $CH_2$: | 24.2 (o), 28.0 (o) | [a] |
| | | (CH)diene (C-1, C-4): | 70.1 (e) | |
| | | (CH)diene (C-2, C-3): | 100.2 (e) | |

[a] Not detected.

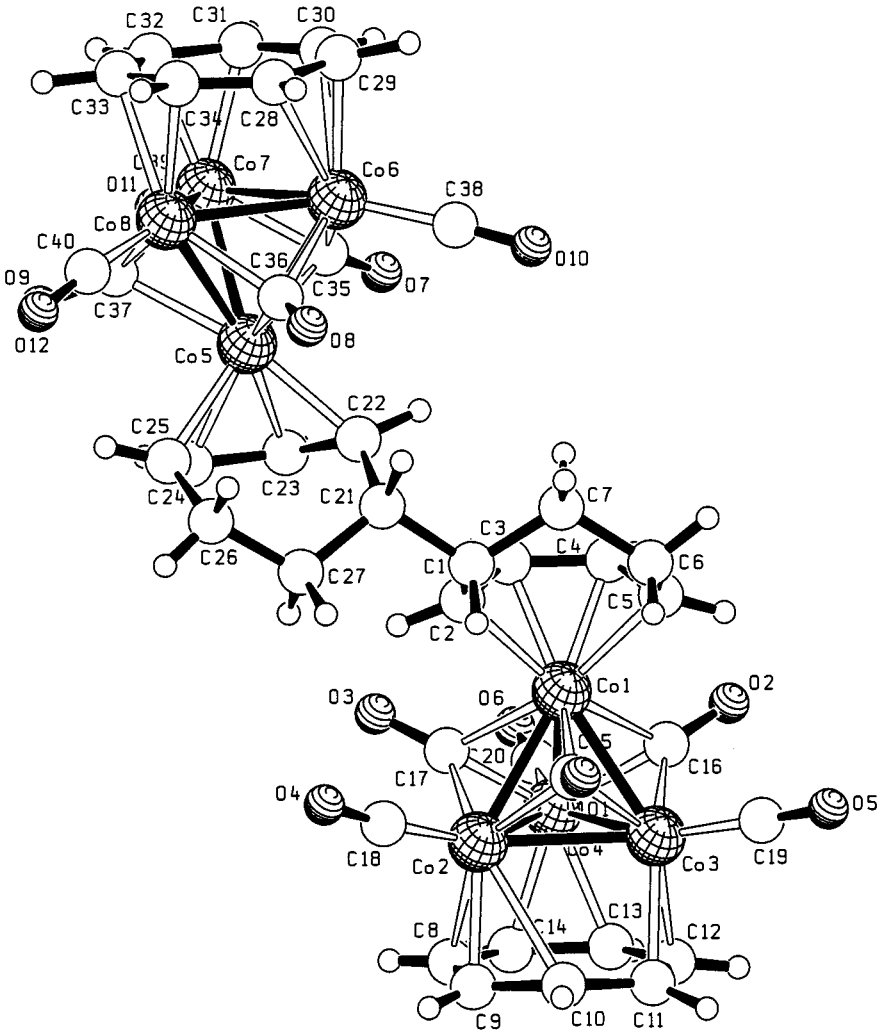


Figure 1. Molecular structure of $[\{Co_4(CO)_3(\mu_3\text{-}CO)_3(\mu_3\text{-}C_7H_7)\}_2\{\mu_2\text{-}\eta^4\text{:}\eta^4\text{-}(C_7H_9)_2\}]^{2-}$ $[\mathbf{4A}]^{2-}$ in the crystals of $[\mathbf{4A}]^{2-}[PPh_4]_2$; only one of the two disordered $\mu_3$-$C_7H_7$ rings bonded to Co6, Co7, and Co8 is shown

anions $[\mathbf{4A}]^{2-}$ consist of two essentially identical subunits of the composition $[Co_4(CO)_3(\mu_3\text{-}CO)_3(\mu_3\text{-}C_7H_7)(C_7H_9)]$, which are fused together through a carbon−carbon bond involving C1 and C21 of the apical $C_7H_9$ ligands.[8] This results in a bridging bicyclic ring system, where both cyclohepta-1,3-diene moieties are $\eta^4$-coordinated to a $[Co_4(CO)_3(\mu_3\text{-}CO)_3(\mu_3\text{-}C_7H_7)]$ cluster unit. With respect to the bridging ligand, the two $Co_4$ clusters adopt an *anti* arrangement. The molecule has approximate $C_2$ symmetry, with the diad bisecting the bond C1−C21.

### Electrochemical Investigations

The anodic cyclic voltammetric (CV) response of the cluster complex $[Co_4(CO)_3(\mu_3\text{-}CO)_3(\mu_3\text{-}C_7H_7)(\eta^5\text{-}C_7H_9)]$ **(3)** in THF solution at a glassy carbon (GC) electrode is similar to those previously reported for the butterfly structure $[Co_4(CO)_{10}(RC_2R)]$,[9] for the binary carbonyls $[Co_4(CO)_{12}]$[10] and $[Co_2(CO)_8]$,[11] and for the organometallic derivatives $[Co_3(CO)_9(CR)]$[12] and $[Co_2(CO)_6(RC_2R)]$.[13] A multi-electron oxidation peak is observed at +0.70 V, followed by an electrochemical response typical of an insoluble material adsorbed onto the electrode, and finally by anodic stripping of metallic Co from the GC electrode. This kind of oxidation process has been described in detail elsewhere[13b] and will not be considered further here. In this study, we focus on reduction processes. The relevant half-wave potentials are summarized in Table 4.

At high scan rates, the cathodic CV response of **3** in THF solution shows two subsequent one-electron processes, centred at $E_{1/2}(A/A') = -0.57$ V and $E_{1/2}(B/B') = -1.22$ V (Figure 2).

The two peak couples, which correspond to the redox processes **3**/$[\mathbf{3}]^-$ (A/A′) and $[\mathbf{3}]^-/[\mathbf{3}]^{2-}$ (B/B′), are electrochemically and chemically reversible. The peak heights are similar to that of the peak due to an equimolar solution of decamethylferrocene (Fc*) added as an internal standard. However, as the scan rate is lowered, chemical complications arise. By switching the potential at −1.00 V, the first one-electron reduction peak couple (A/A′) remains chemically reversible [i.e. the ratio between the anodic (A′) and

Table 3. Selected bond lengths [Å] in $[\{Co_4(CO)_3(\mu_3\text{-}CO)_3(\mu_3\text{-}C_7H_7)\}_2\{\mu\text{-}\eta^4\text{:}\eta^4\text{-}(C_7H_9)_2\}]^{2-}$ **[4A]**$^{2-}$

| | | | |
|---|---|---|---|
| Co1−Co2 | 2.447(2) | Co5−Co6 | 2.456(2) |
| Co1−Co3 | 2.447(2) | Co5−Co8 | 2.439(2) |
| Co1−Co$_4$ | 2.566(1) | Co5−Co7 | 2.545(2) |
| Co2−Co3 | 2.536(2) | Co6−Co8 | 2.536(2) |
| Co2−Co4 | 2.510(2) | Co6−Co7 | 2.501(2) |
| Co3−Co4 | 2.488(2) | Co7−Co8 | 2.505(2) |
| Co1−C15 | 1.912(5) | Co5−C36 | 1.915(6) |
| Co2−C15 | 2.015(5) | Co6−C36 | 2.009(6) |
| Co3−C15 | 2.047(5) | Co8−C36 | 2.022(6) |
| Co1−C16 | 2.190(5) | Co5−C35 | 2.122(6) |
| Co3−C16 | 1.935(6) | Co6−C35 | 1.946(6) |
| Co4−C16 | 1.927(6) | Co7−C35 | 1.927(6) |
| Co1−C17 | 2.147(5) | Co5−C37 | 2.149(6) |
| Co2−C17 | 1.950(6) | Co7−C37 | 1.911(6) |
| Co4−C17 | 1.913(5) | Co8−C37 | 1.944(7) |
| Co−C(CO)term | 1.749(6)−1.752(5) | Co−C(CO)term | 1.738(8)−1.759(6) |
| Co1−C2 | 2.091(5) | Co5−C22 | 2.082(5) |
| Co1−C3 | 2.009(5) | Co5−C23 | 2.012(5) |
| Co1−C4 | 2.010(5) | Co5−C24 | 2.022(5) |
| Co1−C5 | 2.089(5) | Co5−C25 | 2.096(6) |
| Co2−C8 | 2.236(6) | Co3−C12 | 2.155(6) |
| Co2−C9 | 2.032(6) | Co4−C13 | 2.129(6) |
| Co2−C10 | 2.399(7) | Co4−C14 | 2.089(6) |
| Co3−C11 | 2.055(6) | C−C($\mu_3$-$C_7H_7$)[a] | 1.40(1)−1.43(1) |
| C1−C2 | 1.512(7) | C21−C22 | 1.515(7) |
| C1−C7 | 1.522(7) | C21−C27 | 1.529(7) |
| C2−C3 | 1.426(7) | C22−C23 | 1.432(7) |
| C3−C4 | 1.422(7) | C23−C24 | 1.427(7) |
| C4−C5 | 1.416(8) | C24−C25 | 1.416(8) |
| C5−C6 | 1.511(7) | C25−C26 | 1.501(8) |
| C6−C7 | 1.524(7) | C26−C27 | 1.518(7) |
| C1−C21 | 1.570(6) | | |

[a] The non-disordered ring bonded to Co2, Co3 and Co4.

Table 4. Half-wave potentials, $E_{1/2}$ [V], for $[\{Co_4(CO)_3(\mu_3\text{-}CO)_3(\mu_3\text{-}C_7H_7)\}_2\{\mu\text{-}(C_7H_9)_2\}]^{2-}$ **[4]**$^{2-}$ at a dropping mercury electrode in THF and $CH_2Cl_2$

| | A/A′ | B/B′ | C/C′ | D/D′ | E/E′ |
|---|---|---|---|---|---|
| THF | −0.57 | −1.22 | −0.12 | −1.69 | −2.22 |
| $CH_2Cl_2$ | −0.76 | −1.34 | −0.27 | −1.75 | [a] |

[a] Hidden by solvent discharge.

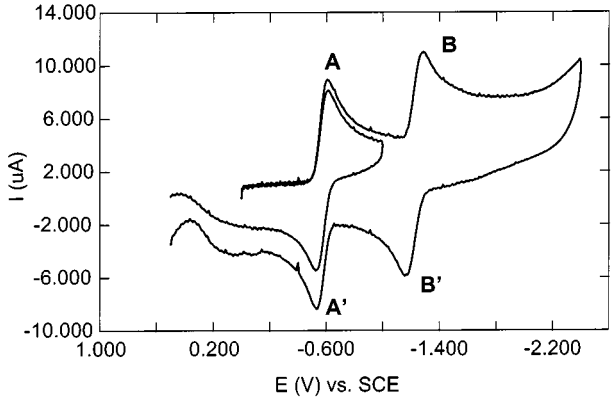


Figure 2. CV response of a THF solution of **3** at a GC electrode (scan rate 8 V s$^{-1}$)

cathodic (A) peak currents, $i_p^a/i_p^c$, is unity] only at scan rates higher than 2 V/s. At lower scan rates, a new species is produced upon reoxidation at peak C′, giving rise to a reversible peak system C/C′ centred at $E_{1/2}$(C/C′) = −0.12 V. New peak systems are seen on scanning in the available cathodic window (up to −2.4 V) at $E_{1/2}$(D/D′) = −1.69 V and $E_{1/2}$($E$/$E$′) = −2.22 V (Figure 3).

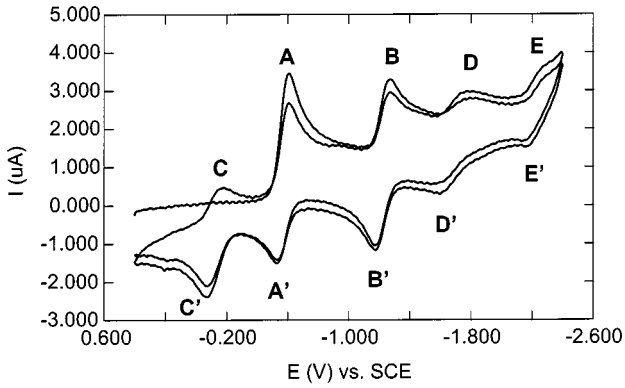


Figure 3. CV response of a THF solution of **3** at a GC electrode (scan rate 0.4 V s$^{-1}$)

Surprisingly, the ratio $i_p^a$(B′)/$i_p^c$(B) is higher than unity at scan rates lower than 2 V/s. Furthermore, the heights of all the observed peaks are lower than $i_p^c$(A). This is particularly evident at low scan rates (e.g. 100 mV/s, see Figure 4). It is interesting to note that even at very low scan rates, $i_p^a$(B′) does not disappear.

FT-IR spectroelectrochemistry (CO stretching region) performed in an OTTLE cell during the first reduction process shows a quantitative chemical conversion of **3** (νCO = 1980, 1730 cm$^{-1}$) to the "dimeric" dianion **[4]**$^{2-}$ ($\nu_{CO}$ = 1925, 1675 cm$^{-1}$), as verified by comparison with the IR spectrum of an authentic sample. Isosbestic points at 1957

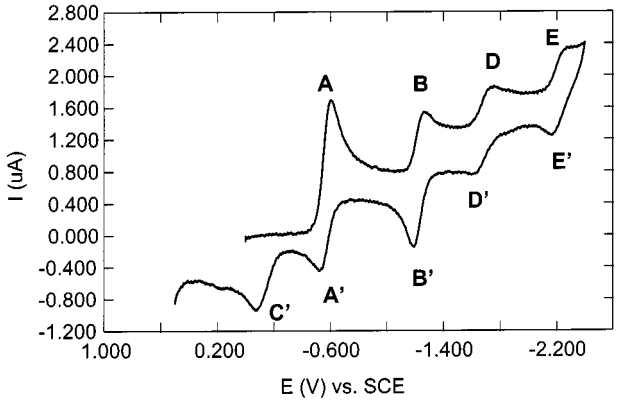


Figure 4. CV response of a THF solution of **3** at a GC electrode (scan rate 0.1 V $s^{-1}$)

$cm^{-1}$ and 1705 $cm^{-1}$ are indicative of full conversion to the dimer in the course of the electrolysis (Figure 5). Reoxidation at the platinum electrode of the OTTLE cell completely restores the original spectrum of the parent compound **3**, suggesting complete chemical reversibility of the system over long-term electrolysis as well.

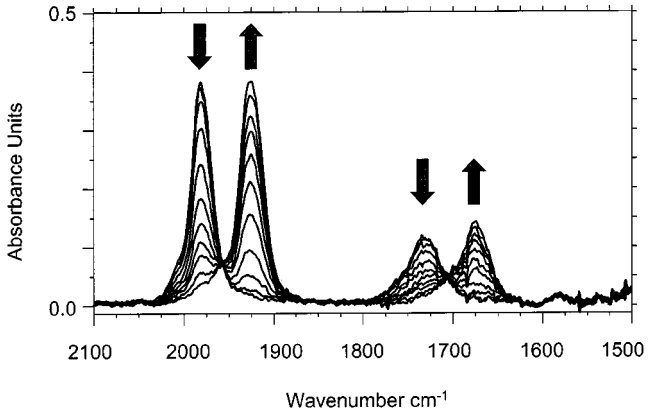


Figure 5. IR OTTLE spectra of a THF solution of **3** during the exhaustive reduction at $E_{app} \approx -0.8$ V

In analogy to CV, polarography of **3** (Figure 6, solid line) shows two reduction waves, A and B. At mercury, a further, very cathodic, reduction process is observed (wave F). Exhaustive electrolysis at a mercury-pool electrode ($E_{appl} = -0.8$ V) was followed by in situ polarography. As 1 F/mol was consumed, waves A and B completely disappeared and an apparent one-electron anodic oxidation wave C and two one-electron reduction waves D and E appeared (dotted line). Re-oxidation at potentials more positive than wave C did not fully restore the original cluster **3** as in OTTLE, probably due to interactions of the cobalt carbonyls with the mercury pool during re-oxidation. Such interactions of cobalt carbonyl derivatives with mercury have been observed several times,[14,15] and have been investigated in detail for the fragment $[Co(CO)_4]^-$.[16]

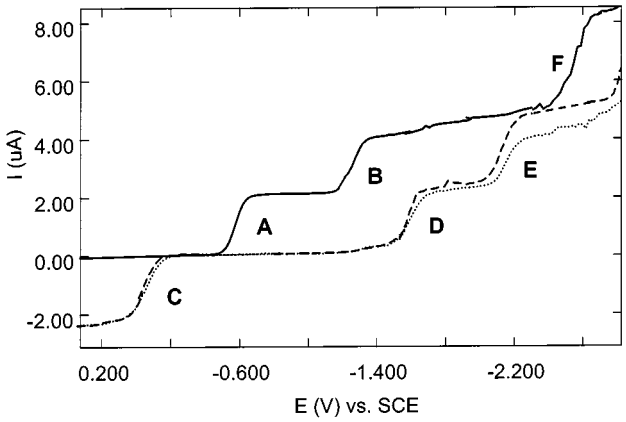


Figure 6. Polarographic responses of a THF solution of **3** recorded in situ during exhaustive electrolysis at a mercury-pool electrode; the solid line corresponds to the initial solution, while the dotted curve was recorded after 1 F/mol had been consumed at $E_{app} \approx -0.8$ V; the dashed curve is the polarographic response of a THF solution of an authentic sample of $[\mathbf{4}]^{2-}$

A pure sample of the dimer $[\mathbf{4}]^{2-}$ (the 86:14 mixture of isomers $[\mathbf{4A}]^{2-}$ and $[\mathbf{4B}]^{2-}$) (dashed line) was found to exhibit the same electrochemical behaviour. The redox waves of $[\mathbf{4}]^{2-}$ (i.e. D and E) are twice the height compared to that of an equimolar solution of Fc*, added as an internal standard. The electron stoichiometry (2 electrons) of both reduction processes was confirmed by coulometry. Furthermore, the polarographic slopes obtained from log-plot analyses and the $\Delta E_p$ values from the CV (both roughly 60 mV) are typical of a single-electron Nernstian process. Waves D and E assigned to $[\mathbf{4}]^{2-}$ (produced by exhaustive electrolysis of **3**) relate to two-electron processes, but correspond to half concentrations of the electroactive species, and therefore their heights are equal to those of waves A and B (assigned to the parent cluster **3**). Finally, $[\mathbf{4}]^{2-}$ exhibits the usual multi-electron chemical irreversible oxidation peak at +0.70 V at glassy carbon.

## Discussion

A family of isoelectronic tetracobalt carbonyl cluster complexes exists where one face of the $Co_4$ tetrahedron is capped by a facial ($\mu_3$) ligand. These include $[Co_4(CO)_6(\mu_2\text{-}CO)_3(\mu_3\text{-trithiane})]$ **(7)**,[17] $[Co_4(CO)_6(\mu_2\text{-}CO)_3\{\mu_3\text{-}HC(EPh_2)_3\}]$ **(8a)** (E = P), **(8b)** (E = As),[18] $[Co_4(CO)_3(\mu_3\text{-}CO)_3(\mu_3\text{-}C_8H_8)(L)]$ **(1)**,[5] and $[Co_4(CO)_3(\mu_3\text{-}CO)_3(\mu_3\text{-}C_7H_7)(L)]$ [L = $\eta^5$-$C_7H_9$ (**3**); $\eta$-$C_5R_5$, R = H, Me].[5] These derivatives of the parent binary carbonyl $[Co_4(CO)_{12}]$ are "electron precise" (60 valence electrons [VE]).[19] It has been demonstrated that the facial ligands tend to stabilize the tetrahedral $Co_4$ cluster core, resulting in a considerably reduced tendency to fragment during the course of chemical and electrochemical reactions. For example, $[Co_4(CO)_{12}]$ readily undergoes complete fragmentation when reduced in the absence of reactants.[6] The one-electron reduction product of **8a**, $[Co_4(CO)_9\{\mu_3\text{-}HC(PPh_2)_3\}]^-$ $[\mathbf{8a}]^-$, is more stable, but undergoes rapid ligand exchange at the apical

cobalt atom.[6b] The cyclooctatetraene-bridged clusters **1** have been shown to undergo pseudo-reversible electrochemical one-electron reductions, but are quantitatively converted to the stable trinuclear anion $[Co_3(CO)_3(\mu_2\text{-}CO)_3(\mu_3\text{-}C_8H_8)]^-$ $[\mathbf{2}]^-$ upon chemical reduction.[4]

A similar behaviour was expected of the cycloheptatrienyl-bridged cluster complexes **3**, from which we hoped to generate the trinuclear dianion $[Co_3(CO)_6(\mu_3\text{-}C_7H_7)]^{2-}$ $[\mathbf{9}]^{2-}$. However, our electrochemical studies have not produced any evidence for the formation of this species. The initial reduction product $[\mathbf{3}]^-$ is indeed transient, but further reaction occurs through intermolecular ligand−ligand coupling to give $[\mathbf{4}]^{2-}$, and not by degradation of the metal framework. With some caution,[20] this can be taken as evidence that the unpaired electron in $[\mathbf{3}]^-$ is essentially centred on the apical $C_7H_9$ ligand, and less so on the metal cluster. This view is also consistent with the formation of minor amounts of $[\mathbf{5}]^-$, which is the electron-precise product of hydrogen abstraction from the solvent or water by $[\mathbf{3}]^-$.

The formation of $[\mathbf{4}]^{2-}$ is regiospecific [carbon−carbon bond formation occurs exclusively at the carbon atom(s) in the enylic positions, adjacent to the unsaturated π-system of the $C_7H_9$ ligand], but not stereospecific. The absolute configuration (*R*,*R*) [and (*S*,*S*)] can be assigned to the bridgehead carbon atoms C1 and C21 in $[\mathbf{4A}]^{2-}$ on the basis of our structure determination. It seems likely that $[\mathbf{4B}]^{2-}$ is the achiral (*R*,*S*) isomer (*meso* form).

The formation of the $Co_3Ru$ complex **6**, another electron-precise cluster, is more difficult to explain. It could be due to a stacking reaction of the ruthenium benzene reagent with the trinuclear dianion $[\mathbf{9}]^{2-}$, akin to the reaction of $[\mathbf{2}]^-$ with $[(\eta\text{-}C_5Me_5)Ru(NCMe)_3]^+$.[4] However, this would require that $[\mathbf{9}]^{2-}$ be present, at least in minor amounts, in the mixture of reduction products of **3**. The paramagnetism of the main product, $[\mathbf{3}]^-$, could prevent the detection of $[\mathbf{9}]^{2-}$ (expected to be diamagnetic) in the reaction mixture by NMR spectroscopy. This interpretation could explain the observation that formation of **6** is complete within a few minutes, whereas the subsequent dimerization of $[\mathbf{3}]^-$ is much slower.

Alternatively, a redox condensation of the tetranuclear $[\mathbf{3}]^-$ with $[(\eta\text{-}C_6H_6)Ru(NCMe)_3]^{2+}$ could take place, which would involve extrusion of a cobalt vertex. Here, the low yield of product **6** would be accounted for by the charge balance, which requires sacrifice of two molecules of $[\mathbf{3}]^-$ for the formation of one molecule of **6**.

A 60 VE count is attained by either of the two $Co_4$ cluster units in $[\mathbf{4A}]^{2-}$, as well as by $[\mathbf{5}]^-$. Hence, the uptake of an electron by **3**, followed by dimerization or hydrogen abstraction, is accompanied by a decrease of hapticity of the apical seven-membered ring ligand (from $\eta^5$ to $\eta^4$). The lengths of the endocyclic carbon−carbon bonds within the bridging $(C_7H_9)_2$ ring system conform to the pattern expected for $\eta^4$-cycloheptadiene ligands: they are shorter within the $\eta^4$-diene systems (mean value 1.42 Å) and longer in the remaining rings (mean value 1.52 Å). The bond C1−C21, which joins the two seven-membered rings, is slightly longer [1.570(6) Å] than would be expected for a single bond. This value compares well with the corresponding bond lengths in the dinuclear complexes $[\{(CO)_3Fe\}_2\{\mu\text{-}\eta^4\text{:}\eta^4\text{-}(C_7H_9)_2\}]$ [1.564(4) Å][21] and $[\{(\eta\text{-}C_5H_5)Co\}_2\{\mu\text{-}\eta^4\text{:}\eta^4\text{-}(C_7H_9)_2\}]$ **(10)** [1.564(5) Å].[22]

Within the limitations of the experimental accuracy, the geometry of the $Co_4(CO)_6$ cluster units in $[\mathbf{4A}]^{2-}$ is quite similar to that seen in other complexes containing the $Co_4(CO)_6(\mu_3\text{-}C_nH_n)$ moiety.[5] The coordination mode of the facial $C_7H_7$ rings approaches the $\mu_3\text{-}\eta^2\text{:}\eta^2\text{:}\eta^3$ fashion and is therefore slightly different from the $\mu_3\text{-}\eta^2\text{:}\eta^3\text{:}\eta^3$ coordination found in **3**.[5] However, owing to the small actual geometric differences between the various forms of the $\mu_3\text{-}\eta^7$ coordination mode, the experimental inaccuracies, and the low barrier to rotation, no great significance should be attached to this observation.

As expected, a high mobility of the facial $C_7H_7$ ligands in $[\mathbf{4}]^{2-}$, $[\mathbf{5}]^-$, and **6** is evident in solution, which can be explained in terms of rapid rotation of the seven-membered rings within their coordination planes. The $^1H$ and $^{13}C$ NMR chemical shifts of these ligands compare well with those observed in **3**.[5] It appears that a $^{13}C$ chemical shift of about $\delta = 60$ is typical for a $C_7H_7$ ligand facially coordinated to a $Co_3$ cluster face, with a minor high-field shift of about 5 ppm when the molecule bears a negative charge. This is in contrast to the much larger coordination shifts that have been reported for $Ru_3(\mu_3\text{-}C_7H_7)$ moieties [$\delta(^{13}C) \approx 39$].[23] The proton resonance of the $\eta^6$-benzene ligand in **6** appears at a chemical shift comparable to that found for apical benzene ligands in hexa- and pentanuclear ruthenium and mixed ruthenium osmium carbonyl cluster complexes.[24] Interestingly, resonances at higher field are observed when the $(\eta\text{-}C_6H_6)Ru$ moiety is part of a penta- or hexanuclear iron carbonyl cluster {e.g. $[Ru(\eta\text{-}C_6H_6)Fe_5C(CO)_{14}]$, $\delta(^1H) = 4.37$; $[Ru(\eta\text{-}C_6H_6)Fe_4C(CO)_{12}]$, $\delta(^1H) = 4.85$}.[25]

The electrochemical data can be accounted for by the mechanism depicted in Scheme 1.

The dimerization of the radical anion $[\mathbf{3}]^-$ to form $[\mathbf{4}]^{2-}$ explains the reversible re-oxidation C′. Interestingly, the oxidized form **4** is unstable in the long-term and decomposes back to **3** almost quantitatively. The dimerization reaction $[\mathbf{3}]^- + [\mathbf{3}]^- \rightarrow [\mathbf{4}]^{2-}$ is sufficiently fast to produce peaks D/D′ and E/E′ (Figure 3), attributable to further reduction of the dimer itself, but not so fast as to lead to complete loss of peaks B and A′ (Figure 4), assigned to further reduction and re-oxidation of the monomer $[\mathbf{3}]^-$, respectively. This justifies the differences in the peak heights discussed above. Contrasting behaviour, where the anomalous peak height was rationalized in terms of a catalytic mechanism, has been observed in a study of the electron-transfer chain reaction that follows the reduction of $[H_4Ru_4(CO)_{12}]$.[26] It is noteworthy that the dianion $[\mathbf{3}]^{2-}$ is much more stable than the monoanion $[\mathbf{3}]^-$ on the CV time scale. This accounts for the fact that $i_p^a(B')$ is higher than $i_p^c(B)$.

The redox behaviour of $[\mathbf{4}]^{2-}$, as outlined above, suggests that the two redox-active moieties, $Co_4(CO)_3(\mu_3\text{-}CO)_3(\mu_3\text{-}C_7H_7)(\eta^4\text{-}C_7H_9)$, directly bonded by a single

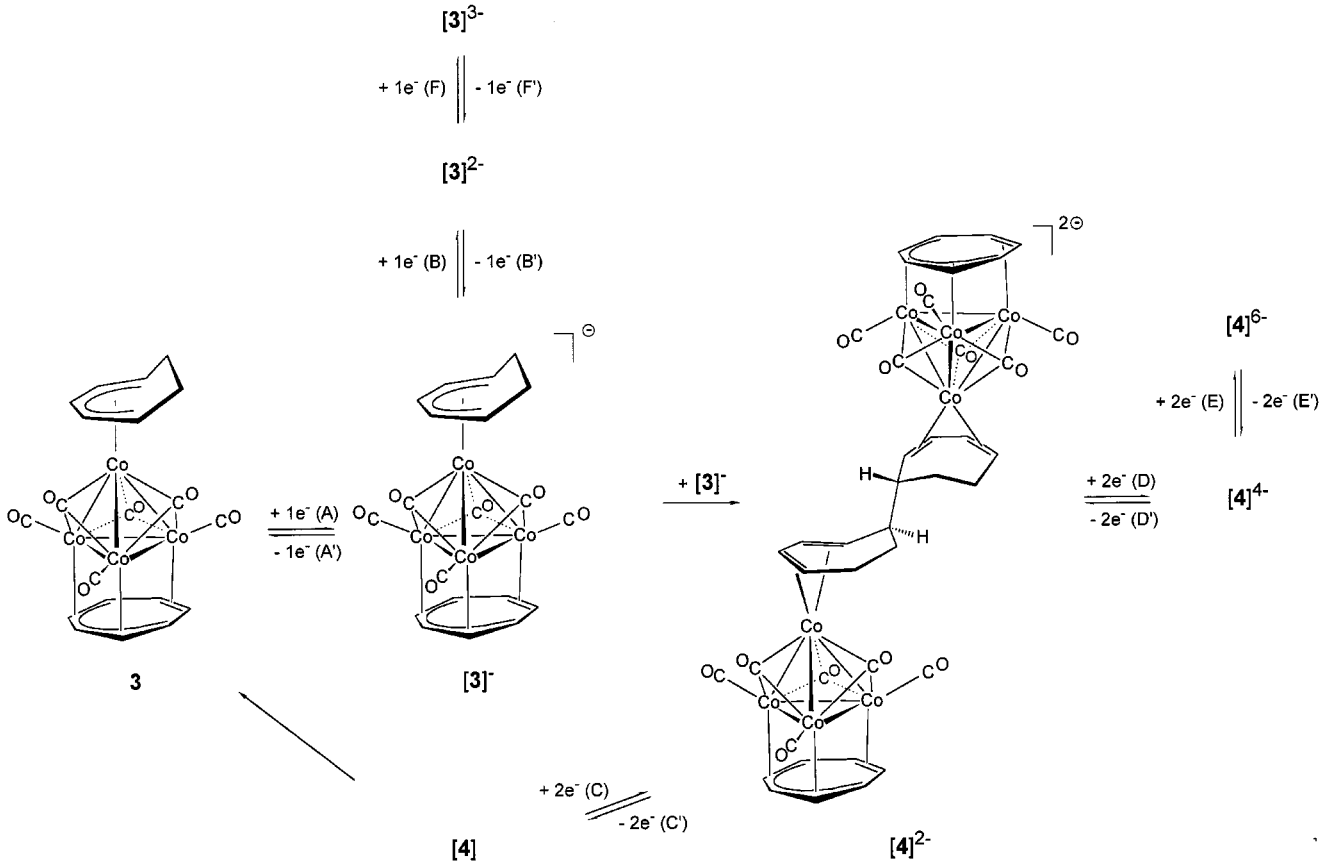


Scheme 1. Redox processes involving complexes **3** and **4**

carbon−carbon bond, act as two independent, non-interacting redox centres. For such a case, the two one-electron reduction processes are separated by 36 mV (statistical factor) and a single, double-height wave is expected.[27]

Digital simulation[28] (Figure 7) of the overall mechanism produced a shape similar to that observed experimentally (Figure 4). The homogeneous rate constant for the dimerization was evaluated as $k_{DIM}$ (2 [**3**]$^-$ → [**4**]$^{2-}$) = 0.30 ± 0.05

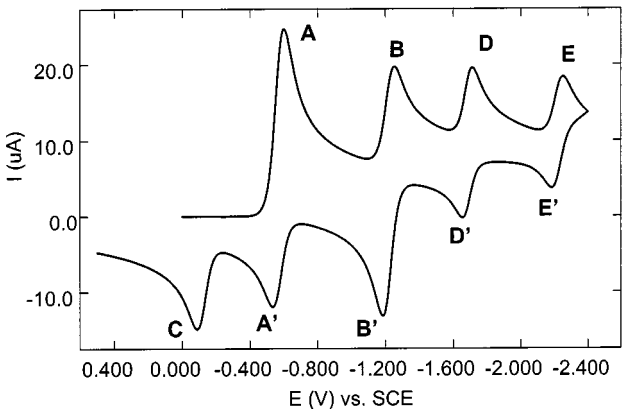


Figure 7. Digital simulation according to the mechanism in Scheme 1; scan rate 0.1 V s$^{-1}$; heterogeneous rate constant ($k°$) = 2 cm s$^{-1}$; α = 0.5; D(**3**) = 1 × 10$^{-5}$ cm$^2$ s$^{-1}$; D(**4**) = 7 × 10$^{-6}$ cm$^2$ s$^{-1}$; $E_{1/2}$(A/A′) = $E_{1/2}$(**3**/[**3**]$^-$) = −0.57 V; $E_{1/2}$(B/B′) = $E_{1/2}$([**3**]$^-$/[**3**]$^{2-}$) = −1.22 V; $E_{1/2}$(**4**/[**4**]$^-$) = −0.102 V; $E_{1/2}$([**4**]$^-$/[**4**]$^{2-}$) = −0.138 V; $E_{1/2}$([**4**]$^{2-}$/[**4**]$^{3-}$) = −1.672 V; $E_{1/2}$([**4**]$^{3-}$/[**4**]$^{4-}$) = −1.698 V; $E_{1/2}$([**4**]$^{4-}$/[**4**]$^{5-}$) = −2.202 V; $E_{1/2}$([**4**]$^{5-}$/[**4**]$^{6-}$) = −2.238 V; $k_f$ (**4** → 2 **3**) = 0.2 s$^{-1}$; $k_{DIM}$ (2 [**3**]$^-$ → [**4**]$^{2-}$) = 0.30 mM$^{-1}$ s$^{-1}$

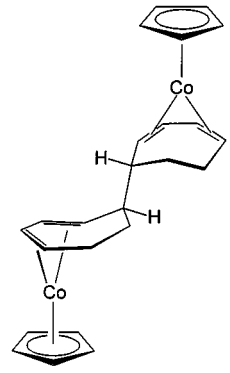


**10**

mM$^{-1}$ s$^{-1}$ (according to the DIM 1 mechanism proposed by Saveant et al.[29]), either by means of best-fitting of the experimental data[28] or by applying the method of Lasia[30] with different values for the scan rates (0.05−1 V/s) and concentrations of **3** (0.6−3 mM). The CV switching potential was 300 mV past the first cathodic peak potential.[30] Both methods gave a similar rate, but simulation produces an "*ad hoc*" working curve.

The redox-induced intermolecular coupling of the two cycloheptadienyl ligands has a precedent in mononuclear chemistry. Geiger et al.[22] observed that [(η-$C_5H_5$)Co(η$^5$-$C_7H_9$)]$^+$ undergoes two reductions, at −0.8 and −1.9 V, the latter process being irreversible. This complex generated the

"dimer" $[\{(\eta\text{-}C_5H_5)Co\}_2\{\mu\text{-}\eta^4\text{:}\eta^4\text{-}(C_7H_9)_2\}]$ **(10)** upon electrolysis at −1.0 V. The value found for the dimerization of the mononuclear cobalt complex ($k_{DIM}$ = 1.35 $mM^{-1}$ $s^{-1}$)[31] is somewhat higher than that found in the present work; this is probably due to the presence of the bulkier tetracobalt unit in **3**. Whereas the dimer **10** is oxidized in two one-electron steps with limited electronic communication, the oxidation of $[\mathbf{4}]^{2-}$ occurs in a single two-electron step. Interestingly, dimer **10** is stable, whereas dimer **4** undergoes spontaneous fission of the newly formed C−C bond, thus constituting the basis of a very interesting redox cycle (see Conclusion).

For **10**, there was no indication that two stereoisomers had been formed. In the crystal used for the structure determination, the same (*R*,*R*) and (*S*,*S*) configurations of the bridgehead carbons as in $[\mathbf{4A}]^{2-}$ were found.

## Conclusion

The propensity of cluster **3** to dimerize upon reduction to $[\mathbf{4}]^{2-}$ with the formation of an additional C−C bond and its reoxidation to **4**, which, in turn, is unstable and spontaneously reverts to **3** in a perfectly reversible manner by cleavage of this C−C bond, constitutes a very promising redox cycle. This system approaches the concept of a "molecular battery" proposed by Floriani,[32] i.e. a molecular device capable of storing and releasing pairs of electrons through the formation and cleavage of chemical bonds. This reservoir of electrons controlled by the reversible formation of C−C bonds may represent an interesting device for electrical energy storage.

## Experimental Section

**General Procedures:** All operations were carried out under an atmosphere of purified nitrogen or argon (BASF R3−11 catalyst) using Schlenk techniques. Solvents were dried by conventional methods. Alumina used as a stationary phase for column chromatography was heated to 180−200 °C in vacuo for several days, deactivated with 5% water, and then stored under nitrogen. The cluster complex **3** was prepared as described previously.[5] NMR spectra were recorded on Bruker AC 200 and AVANCE DRX200 instruments (200.1 MHz for $^1H$, 50.3 MHz for $^{13}C$); $^1H$ and $^{13}C$ chemical shifts are reported *vs.* $SiMe_4$ and were determined by reference to internal $SiMe_4$ or residual solvent peaks. Infrared spectra were recorded from samples in $CaF_2$ cells on a Bruker IFS-28 Fourier-transform spectrometer (optical resolution 0.5 $cm^{-1}$). Elemental analyses were performed locally at the Microanalytical Laboratory of the Organisch-chemisches Institut der Universität Heidelberg and at the Mikroanalytisches Labor Beller, Göttingen.

**$[PPh_4]_2[\{Co_4(CO)_3(\mu_3\text{-}CO)_3(\mu_3\text{-}C_7H_7)\}_2\{\mu_2\text{-}(C_7H_9)_2\}]$ ($[PPh_4]_2[\mathbf{4}]^{2-}$):** A mixture of $[Co_4(CO)_3(\mu_3\text{-}CO)_3(\mu_3\text{-}C_7H_7)(\eta^5\text{-}C_7H_9)]$ **(3)** (1.1 g, 1.7 mmol) and $Na_2[Fe(CO)_4]\cdot 3/2$dioxane (0.64 g, 1.9 mmol) was dissolved in THF (50 mL) and the resulting solution was stirred for 30 min. at room temperature. All volatiles were then removed in vacuo, the residue was redissolved in THF (10 mL), and $[PPh_4]Br$ (3.0 g, 7.2 mmol) was added. After stirring for 1 h, the mixture was filtered and the filtrate was concentrated to a small volume. A tenfold excess of methanol was then added to precipitate the product as a mixture of diastereomers $[\mathbf{4A},\mathbf{B}]^{2-}[PPh_4]_2$ (860 mg, 54%). Partial separation of the isomers (about 86% purity for the less soluble $[\mathbf{4A}]^{2-}[PPh_4]_2$; about 80% purity for $[\mathbf{4B}]^{2-}[PPh_4]_2$) could be achieved by repeated recrystallization from THF/methanol or nitromethane. The mother liquor from the first precipitation with methanol was subsequently chromatographed on alumina (deactivated with 5% water, 2.5 × 20 cm). A red band was eluted from the column with $CH_2Cl_2$, from which 20 mg (1%) of $[Co_4(CO)_3(\mu_3\text{-}CO)_3(\mu_3\text{-}C_7H_7)(C_7H_{10})][PPh_4]$ ($[\mathbf{5}]^-[PPh_4]$) was isolated.

**$[\mathbf{4}]^{2-}[PPh_4]_2$:** IR ($CH_2Cl_2$): ν(CO) = 1955 (sh), 1926 (vs), 1702 (sh), 1675 (s) $cm^{-1}$. − $C_{88}H_{72}Co_8O_{12}P_2$ (1854.96): calcd. C 56.98, H 3.91; found C 56.43, H 4.10.

**$[Co_4(CO)_3(\mu_3\text{-}CO)_3(\mu_3\text{-}C_7H_7)(C_7H_{10})][PPh_4]$ ($[\mathbf{5}]^-[PPh_4]$):** A sample of **3** (270 mg, 0.46 mmol) in THF (30 mL) was treated with 0.5 mL of a 1 M solution of $Li[HBEt_3]$ in THF. After stirring for 30 min. at room temperature, all volatiles were removed in vacuo. The residue was redissolved in THF (5 mL) and to this solution, a solution of $[N\mathit{n}Bu_4]Cl$ (2.4 g, 8.6 mmol) in water (40 mL) was added dropwise. After stirring for 30 min., the product was collected on a glass frit, washed with $H_2O$, toluene, and pentane, and dried in vacuo. Recrystallization from ethanol gave 100 mg (26%) of $[\mathbf{5}]^-[N\mathit{n}Bu_4]$. − IR ($CH_2Cl_2$): ν(CO) = 1955 (sh), 1925 (vs), 1700 (sh), 1675 (s) $cm^{-1}$.

**$[Ru(\eta\text{-}C_6H_6)Co_3(CO)_3(\mu_3\text{-}CO)_3(\mu_3\text{-}C_7H_7)]$ (6):** A 1.6 mL aliquot of a 1 M solution of $Li[HBEt_3]$ in THF was added to a solution of **3** (0.92 g, 1.6 mmol) in THF (50 mL). After stirring for 1 h at room temperature, all volatiles were removed in vacuo. The residue was then treated with a solution of $[(\eta\text{-}C_6H_6)Ru(NCMe)_3][BF_4]_2$ (0.75 g, 1.6 mmol) in $CH_2Cl_2$ (50 mL). After 30 min., some insoluble material was removed by filtration. The filtrate was concentrated to dryness in vacuo, the black residue was washed with *n*-hexane, and then applied to the top of a column (2.5 × 20 cm) of alumina (deactivated with 5% water). Elution with toluene removed a light-brown band from the column. The product was then eluted with $CH_2Cl_2$ as a dark-brown band, from which 180 mg (18%) of black microcrystalline **6** was isolated. − $^1H$ NMR ($CD_2Cl_2$): δ = 3.20 (s, 7 H, $C_7H_7$), 5.35 (s, 6 H, $C_6H_6$). − $^{13}C\{^1H\}$ NMR ($C_6D_6$): δ = 59.8 ($C_7H_7$), 95.6 ($C_6H_6$). − IR (toluene): ν(CO) = 2000 (sh), 1973 (vs), 1715 (s) $cm^{-1}$. − $C_{19}H_{13}Co_3O_6Ru$ (615.18): calcd. C 37.10, H 2.13; found C 37.16, H 2.76.

**Crystal Structure Determination:** Single crystals of $[\mathbf{4A}][PPh_4]_2\cdot 1.5C_7H_8$ were grown from a solution of the 86:14 mixture of isomers $[\mathbf{4A}]^{2-}/[\mathbf{4B}]^{2-}$ in $CH_2Cl_2$ by layering with toluene at room temperature. Intensity data were collected on a Siemens-Stoe AED2 four-circle diffractometer at low temperature (Table 5). The structure was solved by direct methods and refined by full-matrix least-squares based on $F^2$ using all measured unique reflections. One of the $\mu_3\text{-}C_7H_7$ ligands, a phenyl ring in one of the $[PPh_4]^+$ cations, and a toluene solvate molecule were found to be disordered. Most non-hydrogen atoms were given anisotropic displacement parameters, except those of the disordered $C_7H_7$ and toluene rings. Some of the hydrogen atoms were localized in difference Fourier syntheses and were refined isotropically. The remaining hydrogen atoms were placed in calculated positions (except those of the disordered toluene).[33] The calculations were performed using the programs SHELXS-86 and SHELXL-97.[34] Graphical representations were produced using SCHAKAL-92.[35]

Table 5. Details of the crystal structure determination of $[\{Co_4(CO)_3(\mu_3\text{-}CO)_3(\mu_3\text{-}C_7H_7)\}_2\{\mu\text{-}\eta^4\text{:}\eta^4\text{-}(C_7H_9)_2\}][PPh_4]_2\cdot 1.5C_7H_8$ ($[4A]^{2-}$-$[PPh_4]_2$)

| | |
|---|---|
| Formula | $C_{88}H_{72}Co_8O_{12}P_2\cdot 1.5C_7H_8$ |
| Crystal system | triclinic |
| Space group | *P*-1 |
| *a* [Å] | 16.216(9) |
| *b* [Å] | 16.321(9) |
| *c* [Å] | 16.800(9) |
| α [°] | 90.15(4) |
| β [°] | 98.00(4) |
| γ [°] | 104.37(4) |
| *V* [Å$^3$] | 4262(4) |
| *Z* | 2 |
| $M_r$ | 1993.03 |
| $d_c$ [gcm$^{-3}$] | 1.553 |
| $F_{000}$ | 2034 |
| μ(Mo-$K_\alpha$) [mm$^{-1}$] | 1.62 |
| X-radiation, λ [Å] | Mo-$K_\alpha$, graphite-monochromated, 0.71073 |
| Data collect. temp. [°C] | −70 |
| 2θ range [°] | 3−50 |
| *hkl* ranges | $-19 \le h \le 18$<br>$-19 \le k \le 19$<br>$0 \le l \le 19$ |
| Reflections measured | |
| Unique | 15007 |
| Observed [$I \ge 2\,\sigma(I)$] | 10706 |
| Parameters refined | 1197 |
| *R* values | |
| *R* (obsd. reflections only) | 0.053 |
| w*R*2 (all reflections) | 0.143 |
| $(w = 1/[\sigma^2(F)+(A\cdot P)^2+B\cdot P]$, | |
| *A*, *B* | 0.0655, 6.87 |
| *P* | $\max[(F_o^2, 0) + 2\,F_c^2]/3$ |
| GooF | 1.023 |
| Largest/smallest peak in Fourier [eÅ−3] | 0.89/−0.59 |

**Electrochemistry:** THF was distilled from sodium benzophenone ketyl immediately prior to use. Tetrabutylammonium hexafluorophosphate (Aldrich) was recrystallized three times from 95% ethanol and dried in a vacuum oven at 110 °C overnight. Electrochemistry was performed with an EG&G PAR 273 electrochemical analyser connected to a PC, employing the software M270. A standard three-electrode cell was designed to allow the tip of the reference electrode to closely approach the working electrode. The reference used was the Standard Calomel Electrode (SCE). The working electrode for CV was composed of glassy carbon (GC); for polarography, a dropping mercury electrode (DME) with flow rate of 1.22 mg s$^{-1}$ at a reservoir height of 0.5 m was employed. Drop time (typically 1 s) was controlled by an electromechanical hammer. A platinum wire served as the auxiliary electrode. Positive feedback *iR* compensation was applied routinely. All measurements were carried out under Ar in anhydrous deoxygenated THF or $CH_2Cl_2$. Solutions were $5 \times 10^{-4}$ M in the compounds under study and $1 \times 10^{-1}$ M in the supporting electrolyte, $[Bu_4N][PF_6]$. Since the oxidation process of ferrocene (Fc) overlaps with those of the compounds under study, we employed decamethylferrocene (Fc*) as an internal standard; the Fc*(0/1+) potential was evaluated as +0.11 V *vs.* SCE in THF.[36,37] The number of electrons transferred ($n_{app}$) in a particular redox process was determined by controlled potential coulometry at a mercury pool. Each experiment was carried out in duplicate. Spectroelectrochemistry was performed in an optically transparent thin-layer electrochemical (OTTLE) cell assembled as described previously;[38] the spectra were recorded on a Bruker Equinox 55 FT-IR spectrometer.

## Acknowledgments

This work was supported by the Sonderforschungsbereich 247 der Universität Heidelberg, the Fonds der Chemischen Industrie, and MURST (Rome) (COFIN-98). The award of a Heisenberg Fellowship to H.W. is gratefully acknowledged. J.F. thanks the University of Torino for a visiting grant (scambi culturali).

[1] [1a] H. Vahrenkamp, *Adv. Organomet. Chem.* **1983**, *22*, 169. − [1b] W. E. Geiger, N. G. Connelly, *Adv. Organomet. Chem.* **1985**, *24*, 87. − [1c] W. E. Geiger, *Progr. Inorg. Chem.* **1985**, *33*, 275. − [1d] P. Lemoine, *Coord. Chem. Rev.* **1988**, *83*, 169. − [1e] S. R. Drake, *Polyhedron* **1990**, *9*, 455. − [1f] P. Zanello, *Struct. Bonding* **1992**, *79*, 101. − [1g] G. Longoni, C. Femoni, M. C. Iapalucci, P. Zanello, in *Metal Clusters in Chemistry* (Eds.: P. Braunstein, L. A. Oro, P. R. Raithby), Wiley-VCH, Weinheim, **1999**, vol. 2, ch. 3.9.

[2] [2a] N. J. Coville, M. O. Albers, *Coord. Chem. Rev.* **1984**, *53*, 227. − [2b] D. Astruc, *Angew. Chem.* **1988**, *100*, 662.

[3] For examples discussed recently in the literature, see: W. E. Geiger, M. J. Shaw, M. Wünsch, C. E. Barnes, F. H. Foersterling, *J. Am. Chem. Soc.* **1997**, *119*, 2804. M. P. Robben, P. H. Rieger, W. E. Geiger, *J. Am. Chem. Soc.* **1999**, *121*, 367.

[4] H. Wadepohl, S. Gebert, R. Merkel, H. Pritzkow, *Eur. J. Inorg. Chem.* **2000**, in print.

[5] [5a] H. Wadepohl, S. Gebert, H. Pritzkow, D. Braga, F. Grepioni, *Chem. Eur. J.* **1998**, *4*, 279. − [5b] H. Wadepohl, *Coord. Chem. Rev.* **1999**, *185−186*, 551.

[6] [6a]P. Chini, V. Albano, S. Martinengo, *J. Organomet. Chem.* **1969**, *16*, 471. − [6b] J. Rimmelin, P. Lemoine, M. Gross, D. de Montauzon, *Nouv. J. Chem.* **1983**, *7*, 453.

[7] [7a] G. Fachinetti, *J. Chem. Soc., Chem. Commun.* **1979**, 396. − [7b] H.-N. Adams, G. Fachinetti, J. Strähle, *Angew. Chem.* **1980**, *92*, 411.

[8] In this paper, the face of the $M_4$ cluster at which the $\mu_3$-ligand is bound is referred to as the "basal $M_3$ plane". The fourth metal atom and the ligands attached to it are "apical".

[9] D. Osella, M. Ravera, C. Nervi, C. E. Housecroft, P. R. Raithby, P. Zanello, F. Laschi, *Organometallics* **1991**, *10*, 3253.

[10] G. F. Holland, D. E. Ellis, W. C. Trogler, *J. Am. Chem. Soc.* **1986**, *108*, 1884.

[11] Y. Mugnier, P. Reeo, C. Moise, E. Laviron, *J. Organomet. Chem.* **1983**, *254*, 111.

[12] [12a] J. C. Kotz, J. V. Petersen, R. C. Reed, *J. Organomet. Chem.* **1976**, *120*, 433. − [12b] A. M. Bond, B. M. Peake, B. H. Robinson, J. Simpson, D. J. Watson, *Inorg. Chem.* **1977**, *16*, 410.

[13] [13a] M. Arewgoda, P. H. Rieger, B. H. Robinson, J. Simpson, S. J. Visco, *J. Am. Chem. Soc.* **1982**, *104*, 5633. − [13b] D. Osella, E. Stein, G. Jaouen, P. Zanello, *J. Organomet. Chem.* **1991**, *401*, 37.

[14] [14a] D. Osella, L. Milone, C. Nervi, M. Ravera, *J. Organomet. Chem.* **1995**, *488*, 1. − [14b] N. Duffy, J. McAdam, C. Nervi, D. Osella, M. Ravera, B. Robinson, J. Simpson, *Inorg. Chim. Acta* **1996**, 99.

[15] S. W. Blach, A. M. Bond, R. Colton, *Inorg. Chem.* **1981**, *20*, 755.

[16] D. Osella, J. Fiedler, *Organometallics* **1992**, *11*, 3875.

[17] S. Rossi, J. Pursiainen, T. A. Pakkanen, *J. Organomet. Chem.* **1992**, *436*, 55.

[18] [18a] A. A. Bahsoun, J. A. Osborn, C. Voelker, J. J. Bonnet, G. Lavigne, *Organometallics* **1982**, *1*, 1114. − [18b] D. J. Darensbourg, D. J. Zalewski, T. Delord, *Organometallics* **1984**, *3*, 1210. − [18c] D. J. Darensbourg, D. J. Zalewski, A. L. Rheingold, R. L. Durney, *Inorg. Chem.* **1986**, *25*, 3281.

[19] D. M. P. Mingos, D. J. Wales, *Introduction to Cluster Chemistry*, Prentice-Hall, Englewood Cliffs, **1990**, ch. 2.

[20] D. Astruc, *Chem. Rev.* **1988**, *88*, 1189; *Acc. Chem. Res.* **1991**, *24*, 36.

[21] B. Niemar, J. Breimair, B. Wagner, K. Polborn, W. Beck, *Chem. Ber.* **1991**, *124*, 2227.

[22] W. E. Geiger, T. Gennett, G. A. Lane, A. Salzer, A. L. Rheingold, *Organometallics* **1986**, *5*, 1352.

[23] T. A. Cresswell, J. A. K. Howard, F. G. Kennedy, S. A. R. Knox, H. Wadepohl, *J. Chem. Soc., Dalton Trans.* **1981**, 2220.

[24] [24a] P. J. Dyson, B. F. G. Johnson, J. Lewis, M. Martinelli, D. Braga, F. Grepioni, *J. Am. Chem. Soc*. **1993**, *115*, 9062. – [24b] P. J. Dyson, B. F. G. Johnson, D. Reed, D. Braga, F. Grepioni, E. Parisini *J. Chem. Soc., Dalton Trans.* **1993**, 2817. – [24c] D. Braga, P. Sabatino, P. J. Dyson, A. J. Blake, B. F. G. Johnson, *J. Chem. Soc., Dalton Trans.* **1994**, 393. – [24d] J. Wing-Sze Hui, W.-T. Wong, *J. Organomet. Chem.* **1996**, *524*, 211. – [24e] T. Borchert, J. Lewis, P. R. Raithby, G. P. Shields, H. Wadepohl, *Inorg. Chim. Acta* **1998**, *274*, 201.

[25] S. Gebert, Ph.D. Thesis, Universität Heidelberg, **1997**; H. Wadepohl, S. Gebert, unpublished.

[26] D. Osella, C. Nervi, M. Ravera, J. Fiedler, V. Strelets, *Organometallics* **1995**, *14*, 2501.

[27] M. D. Ward, *Chem. Soc. Rev.* **1995**, *24*, 121 and references therein.

[28] The program, ESP (C. Nervi), is available at the URL: http://lem.ch.unito.it/chemistry/esp_manual.html.

[29] [29a] C. P. Andrieux, L. Nadjo, J. M. Saveant, *J. Electroanal. Chem.* **1970**, *26*, 147. – [29b] C. P. Andrieux, L. Nadjo, J. M. Saveant, *J. Electroanal. Chem.* **1973**, *42*, 223.

[30] A. Lasia, *J. Electroanal. Chem.* **1983**, *146*, 413.

[31] W. E. Geiger, personal communication.

[32] E. Gallo, E. Solari, N. Re, C. Floriani, A. Chiesi-Villa, C. Rizzoli, *J. Am. Chem. Soc.* **1997**, *119*, 5144, and references therein.

[33] Crystallographic data (excluding structure factors) for the structure reported in this paper have been deposited with the Cambridge Crystallographic Data Centre as supplementary publication no. CCDC-137254. Copies of the data can be obtained free of charge on application to The Director, CCDC, 12 Union Road, Cambridge CB2 1EZ, U.K. [Fax: (internat.) +44 (0)1223/336033; E-mail: teched@chemcrys.cam.ac.uk].

[34] *SHELXS-86*, G. M. Sheldrick, *Acta Crystallogr.* **1990**, *A46*, 467; *SHELXL-97*, G. M. Sheldrick, Universität Göttingen, **1997**.

[35] *SCHAKAL*-92, E. Keller, Universität Freiburg, **1992**.

[36] U. Kölle, F. Khouzami, *Angew. Chem. Int. Ed. Engl*. **1980**, *19*, 640.

[37] W. E. Geiger, in *Organometallic Radical Processes* (Ed.: W. C. Trogler), Elsevier, Amsterdam, **1990**, ch. 5.

[38] M. Krejcik, M. Danek, F. Hartl, *J. Electroanal.Chem.* **1991**, *317*, 179.

Received November 25, 1999
[I99435]